ELSEVIER

0263-8223(95)00096-8

Composite Structures 33 (1995) 7-15

0263-8223/95/$9.50

Effect of material nonlinearity on buckling and postbuckling of fiber composite laminated plates and cylindrical shells

S. S. Wang, S. Srinivasan

Department of Mechanical Engineering, University of Houston, Houston, TX 77204, USA

H. T. Hu

Department of Civil Engineering, National Cheng-Kung University, Tainan, Taiwan, R.O.C.

&

R. HajAli

Department of Civil Engineering, University of Illinois, Urbana, IL 61801, USA

An analytical study is presented in this paper on the effect of material nonlinearity on buckling and postbuckling of fiber composite laminate plates and shells subjected to general mechanical loading. The material nonlinearity of the composite is modelled by power-law type, nonlinear shear constitutive equations for each lamina. The nonlinear effective composite constitutive equations in an incremental form are incorporated into a geometrically nonlinear analysis for studying buckling and postbuckling deformations of composite laminate structures. A modified Riks' solution scheme with an updated Lagrangian formulation is used to construct the equilibrium path during composite postbuckling. Numerical examples are given to illustrate the effect of material nonlinearity on buckling load, postbuckling stiffness, and associated mode shape change of a composite structure under axial and pressure loading. Influences of lamination parameters, geometric imperfection, and loading mode on the postbuckling equilibrium path and load-bearing strength of the composite structure with the nonlinear material properties are also studied.

1 INTRODUCTION

Advanced fiber composite materials are known to exhibit appreciable shear nonlinearity in their effective ply constitutive equations during deformation. As unidirectional fiber composite laminae are assembled into multilayered composite laminate structures with different ply fiber orientations, discontinuity of material properties through the thickness direction and interaction of the ply material nonlinearity among the composite laminae are expected to introduce significant complexities in the deformation and failure of the composite laminate structures. This situation is of particular concern in buckling and postbuckling of composite laminate plates and shells in which both geometric nonlinearity and material nonlinearity are generally expected to occur and their interactive roles are not yet fully understood.

While buckling is an important consideration in structural design, it is also critical to understand the load-carrying capability and deformations beyond buckling. Numerous studies on these subjects have been reported in the literature for linear isotropic plates, curved panels, and spherical and cylindrical shells with initial geometric imperfections. In the case of fiber composite laminate structures, different lamination variables, such as ply orientations and stacking sequences, lead to widely distinct postbuckling characteristics.[1] As is well known, fiber composite structures, in contrast to their metallic counterparts, may exhibit a high degree of flexibility in shear[2] due to inherent anisotropy and weak shear stiffness. The shear deformation could be further aggravated during buckling and postbuckling processes. Several reviews[1,2] address the issue of buckling of composite laminate plates and shells with linear effective constitutive properties.

Research on the effect of nonlinear effective constitutive material properties on composite structural buckling and postbuckling responses has been very limited. Several approaches at different scale levels have been proposed to model the nonlinear effective constitutive behavior of fiber reinforced composites, e.g., the finite-element micromechanical model based on a unit-cell structure[3] and the macromechanical models based on lamina nonlinear elasticity[4–6] and incremental matrix plasticity.[7,8] With the nonlinear composite constitutive properties, few attempts have been made to study buckling of thin composite laminate panels[9] and postbuckling of thick-section composite laminate plates.[10,11] Owing to the mathematical complexities involved, only recently, limited initial efforts[11–13] have been attempted on geometrically nonlinear postbuckling analyses of cylindrical composite laminate shells with nonlinear shear constitutive properties. The need of a systematic study is obvious for this class of problems on interactions between geometric and material nonlinearities in fiber composite laminate buckling and postbuckling deformations.

The objectives of this paper are to: (1) develop efficient and accurate solution methods to examine the material and geometric nonlinearity interaction problem; (2) investigate effects of composite shear nonlinearity on buckling load, postbuckling stiffness change, mode shapes and imperfection sensitivity of composite laminate structures; and (3) determine effects of various composite laminate variables, structural geometry and loading modes on material nonlinearity and structural instability interaction.

In the next section, an incremental formulation of effective nonlinear composite material constitutive equations at the fiber-composite ply level is introduced first. An efficient algorithm for the incremental formulation is developed and incorporated into a numerical scheme of modeling the nonlinear composite structural response. The updated Lagrangian formulation with a modified Riks' solution scheme is used in Section 2.2 to determine the equilibrium path during composite laminate postbuckling. Numerical examples are given in Section 3 to illustrate the effect of material nonlinearity on geometrically nonlinear buckling and postbuckling behavior of composite laminate plates and shells with various lamination variables. Significant influences of the composite shear nonlinearity on buckling load, postbuckling stiffness and strength, and structural failure modes are obtained for fiber-composite laminate structures under different loading modes.

2 FORMULATION

2.1 Nonlinear constitutive equations for fiber composites

In a fiber-composite laminate, each lamina may be considered as an anisotropic layer in a plane-stress condition. A common stress-strain expression for a linear fiber composite lamina in material coordinates can be written as

$$\{\sigma'\}=[\mathbf{Q}'_1]\{\varepsilon'\} \tag{1}$$

$$\{\tau'_t\}=[\mathbf{Q}'_2]\{\gamma'_t\} \tag{2}$$

where

$$[\mathbf{Q}'_1]=\begin{bmatrix} \dfrac{E_{11}}{1-\nu_{12}\nu_{21}} & \dfrac{\nu_{12}E_{22}}{1-\nu_{12}\nu_{21}} & 0 \\ \dfrac{\nu_{21}E_{11}}{1-\nu_{12}\nu_{21}} & \dfrac{E_{22}}{1-\nu_{12}\nu_{21}} & 0 \\ 0 & 0 & G_{12} \end{bmatrix},$$

$$[\mathbf{Q}'_2]=\begin{bmatrix} \alpha_1 G_{13} & 0 \\ 0 & \alpha_2 G_{23} \end{bmatrix} \tag{3}$$

and $\{\sigma'\}=\{\sigma_1, \sigma_2, \tau_{12}\}^T$, $\{\tau'_t\}=\{\tau_{13}, \tau_{23}\}^T$, $\{\varepsilon'\}=\{\varepsilon_1, \varepsilon_2, \gamma_{12}\}^T$, and $\{\gamma'_t\}=\{\gamma_{13}, \gamma_{23}\}^T$. The constants α_1 and α_2 are shear correction factors and may be taken to be 0·83[11] in this study.

Based on a complementary energy density formulation, the nonlinear constitutive equations for a fiber composite may be written[6] as

$$\begin{Bmatrix}\varepsilon_1\\ \varepsilon_2\\ \gamma_{12}\end{Bmatrix}=\begin{bmatrix}\frac{1}{E_{11}} & -\frac{\nu_{21}}{E_{22}} & 0\\ -\frac{\nu_{12}}{E_{11}} & \frac{1}{E_{22}} & 0\\ 0 & 0 & \frac{1}{G_{12}}\end{bmatrix}\times\begin{Bmatrix}\sigma_1\\ \sigma_2\\ \tau_{12}\end{Bmatrix}+S_{6666}\tau_{12}^2\begin{Bmatrix}0\\ 0\\ \tau_{12}\end{Bmatrix} \quad (4)$$

Note that in the above equations only one material parameter, S_{6666}, is required to account for the in-plane nonlinearity of the composite lamina. By inverting and differentiating eqn (4), an incremental stress-strain relationship of the nonlinear composite is obtained as

$$\Delta\{\sigma'\}=[\mathbf{Q}'_1]\,\Delta\{\varepsilon'\} \quad (5a)$$

where

$$[\mathbf{Q}'_1]=\begin{bmatrix}\frac{E_{11}}{1-\nu_{12}\nu_{21}} & \frac{\nu_{12}E_{22}}{1-\nu_{12}\nu_{21}} & 0\\ \frac{\nu_{21}E_{11}}{1-\nu_{12}\nu_{21}} & \frac{E_{22}}{1-\nu_{12}\nu_{21}} & 0\\ 0 & 0 & \frac{1}{\frac{1}{G_{12}}+3S_{6666}\tau_{12}^2}\end{bmatrix} \quad (5b)$$

2.2 Buckling and postbuckling analyses of fiber composite laminate structures

(a) Method of analysis

The analyses of buckling and postbuckling of fiber-composite laminate plates and shells with geometric imperfections are carried out using the ABAQUS finite element code.[14] The kinematics of large displacements with small strains are incorporated in an updated Lagrangian formulation. In order to model possible snap-through and snap-back deformations, a modified Riks'[15,16] nonlinear incremental algorithm is used to construct the equilibrium path. The solution procedure requires large-scale computations to determine adjacent points along the equilibrium path, from a current solution point on the path, in a space defined by nodal variables and loading parameters. A trial solution is chosen first by moving along the tangent to the equilibrium path of the current solution. The search for the equilibrium path is carried out in the plane which passes through the trial point and is orthogonal to the tangent of the updated solution.

(b) Finite element formulation

Eight-node isoparametric shell elements with six degrees of freedom per node, i.e. three displacements and three rotations, are used for structural discretization. The elements are C° continuous, with Mindlin-type displacement field assumptions which include transverse shear deformations. The displacements $\{u\}$ at a distance z from the composite laminate mid-surface are given as

$$\{u\}=\{u^\circ\}+z[\varphi]\{\beta\} \quad (6)$$

where $\{u^\circ\}$ are mid-surface displacements, $\{\beta\}=\{\beta_2, -\beta_1, 0\}$ are rotations about the triad $\{v_2, v_1, v_3\}$. The orthogonal vectors v_1 and v_2 lie in the plane of the element, and v_3 is normal to the plane of the element. The transformation matrix $[\varphi]$ is defined as

$$[\varphi]=\begin{bmatrix}0 & \theta_{33} & -\theta_{23}\\ -\theta_{33} & 0 & \theta_{13}\\ \theta_{23} & -\theta_{13} & 0\end{bmatrix} \quad (7)$$

where $\theta_{ij}=(e_i\,.\,v_j)$, and e_i are the unit vectors along the global coordinate axes. For a rectangular flat plate with its mid-surface in the x-y plane, β_2 equals to θ_x and $\beta_1=\theta_y$.

The incremental constitutive equations of a composite lamina in the element coordinates can be written as

$$\Delta\{\sigma\}=[\mathbf{Q}_1]\Delta\{\varepsilon\} \quad [\mathbf{Q}_1]=[\mathbf{T}_1]^T[\mathbf{Q}'_1][\mathbf{T}_1] \quad (8)$$

$$\Delta\{\tau_t\}=[\mathbf{Q}_2]\Delta\{\gamma_t\} \quad [\mathbf{Q}_2]=[\mathbf{T}_2]^T[\mathbf{Q}'_2][\mathbf{T}_2] \quad (9)$$

where

$$[\mathbf{T}_1]=\begin{bmatrix}\cos^2\phi & \sin^2\phi & \cos\phi\sin\phi\\ \sin^2\phi & \cos^2\phi & -\sin\phi\cos\phi\\ -2\sin\phi\cos\phi & 2\sin\phi\cos\phi & \cos^2\phi-\sin^2\phi\end{bmatrix},\quad [\mathbf{T}_2]=\begin{bmatrix}\cos\phi\ \sin\phi\\ -\sin\phi\ \cos\phi\end{bmatrix} \tag{10}$$

and $\{\sigma\}=\{\sigma_x,\ \sigma_y,\ \tau_{xy}\}^T$, $\{\tau_t\}=\{\tau_{xz},\ \tau_{yz}\}^T$, $\{\varepsilon\}=\{\varepsilon_x,\ \varepsilon_y,\ \gamma_{xy}\}^T$, $\{\gamma_t\}=\{\gamma_{xz},\ \gamma_{yz}\}^T$, and ϕ is measured counter-clockwise from the element local x-axis to the material 1-axis. The $[\mathbf{Q}'_1]$ matrix used in eqn (8) may be taken from eqn (5b) for the nonlinear formulation. The $\{\varepsilon^0\}=\{\varepsilon_x^{\circ},\ \varepsilon_y^{\circ},\ \gamma_{xy}^{\circ}\}^T$ and $\{\kappa\}$ are in-plane strains and curvatures of the mid-surface of a composite laminate section, respectively. The incremental in-plane strains at a distance z from the mid-surface become

$$\Delta\{\varepsilon\}=\Delta\{\varepsilon^{\circ}\}+z\Delta\{\kappa\} \tag{11}$$

If t is the total thickness of a composite laminate section, the incremental stress resultants of the section can be defined as

$$\Delta\{N\}=\int_{-t/2}^{t/2}[\mathbf{Q}_1](\Delta\{\varepsilon^{\circ}\}+z\Delta\{\kappa\})\,\mathrm{d}z \tag{12a}$$

$$\Delta\{M\}=\int_{-t/2}^{t/2}z[\mathbf{Q}_1](\Delta\{\varepsilon^{\circ}\}+z\Delta\{\kappa\})\,\mathrm{d}z \tag{12b}$$

$$\Delta\{V\}=\int_{-t/2}^{t/2}[\mathbf{Q}_2]\Delta\{\gamma_t\}\,\mathrm{d}z \tag{12c}$$

where $\{N\}=\{N_x,\ N_y,\ N_{xy}\}^T$, $\{M\}=\{M_x,\ M_y,\ M_{xy}\}^T$ and $\{V\}=V_x,\ V_y\}^T$. For a composite laminate with n plies, the incremental laminate constitutive equations at an element integration point can be written as

$$\begin{bmatrix}\Delta\{N\}\\ \Delta\{M\}\\ \Delta\{V\}\end{bmatrix}=\sum_{j=1}^{n}\begin{bmatrix}(z_{jt}-z_{jb})[\mathbf{Q}_1] & \frac{1}{2}(z_{jt}^2-z_{jb}^2)[\mathbf{Q}_1] & [0]\\ \frac{1}{2}(z_{jt}^2-z_{jb}^2\}[\mathbf{Q}] & \frac{1}{3}(z_{jt}^3-z_{jb}^3)[\mathbf{Q}_1] & [0]\\ [0]^T & [0]^T & (z_{jt}-z_{jb})[\mathbf{Q}_2]\end{bmatrix}\begin{Bmatrix}\Delta\{\varepsilon^{\circ}\}\\ \Delta\{\kappa\}\\ \Delta\{\gamma_t\}\end{Bmatrix} \tag{13}$$

where z_{jt} and z_{jb} are distances from the mid-surface of the section to top and bottom surfaces of the j-th ply, respectively. For a general composite laminate plate or shell, extensional and flexural terms are usually coupled. However, if the composite laminate lay-up is symmetric with respect to the mid-surface of the laminate section, the extensional and flexural terms may become uncoupled.

(c) Effect of geometric imperfection

To model bifurcation from a prebuckling to a postbuckling state, a common practice is to introduce geometric imperfections to the initial composite laminate geometry. A small fraction of the eigenmodes corresponding to the lowest n eigenvalues, which are determined by a linearized buckling analysis, is added to the original nodal coordinates of the composite structure, i.e.,

$$\{I\}=\{O\}+\varepsilon t\sum_{i=1}^{n}\{\psi_i\} \tag{14}$$

where $\{I\}$ are resulting nodal coordinates of the structure with the imperfection; $\{O\}$, the original nodal coordinates of the structure; ε is a scaling parameter; t is the thickness of the composite laminate; and ψ_i is the eigenmode corresponding to the i-th lowest eigenvalue. Different values of ε are used in the current study of imperfection sensitivity of the post-buckling response of a composite structure with shear nonlinearity.

(d) Solution accuracy and convergence

Donnell's nonlinear stability theory for shallow shells is used to compute the buckling load and mode shapes of a composite shell with linear constitutive equations. A systematic study has been carried out, using the aforementioned analysis, to evaluate the effect of mesh discretization on the buckling loads and buckling modes of composite shells. The converged solutions are compared with the results obtained from the analytical theory. The information obtained from the converged solutions is used in subsequent postbuckling analyses of composite laminate shells with imperfections.

3 NUMERICAL EXAMPLES

The incremental-iterative solution procedure outlined in Section 2 is used to analyze geometrically nonlinear buckling and postbuckling of fiber-composite laminate plates and shells with nonlinear effective ply constitutive equations. In each case, effects of material nonlinearity on the critical buckling load, postbuckling deformation and stiffness, and the mode shape change are examined. Also, in these coupled geometrically nonlinear and material nonlinear interaction problems, imperfection sensitivity, influences of composite lamination variables, structural geometry and loading modes on composite structural buckling and postbuckling responses are studied.

3.1 Fiber composite laminate plate under uniaxial compression

Consider a $[(0°)/(90°)/(\pm 45°)]_s$ composite laminate plate of planar dimensions $L_x \times L_y$ and thickness t, clamped along all four edges[10] (Fig. 1). The composite plate is subjected to an in-plane uniaxial compression. The geometry of the plate analyzed is given as follows: $L_x = L_y = L = 30$ cm, and $t/L = 0{\cdot}08$. The fiber-reinforced composite material considered in this study is an AS4 carbon-fiber/polyamide thermoplastic-matrix composite with the following effective ply properties: $E_{11} = 123{\cdot}42$ GPa, $E_{22} = 6{\cdot}21$ GPa, $\nu_{12} = 0{\cdot}31$, $G_{12} = G_{13} = 5{\cdot}31$ GPa, $G_{23} = 2{\cdot}14$ GPa, $S_{6666} = 93{\cdot}73$ (GPa)$^{-3}$. The nonlinear shear stress-strain relationship of the composite lamina is shown graphically in Fig. 2 for illustration.

The buckling load and mode shape of the composite laminate under the aforementioned load are obtained from a linear eigenvalue analysis. The mode shapes corresponding to the lowest three eigenvalues are used for introducing the imperfection geometry (eqn 14) with the scaling parameter, ε, being taken as 0·01. The end-shortening vs. loading curves of the composite laminate plate with the linear and nonlinear constitutive properties are shown in Fig. 3. In the figure, the end-shortening, Δu, is normalized by the laminate thickness, t, and the applied nominal load is normalized by the buckling load, $(N_x)_b$, obtained from the linear bifurcation analysis. The end-shortening vs. applied load curves illustrate the inherent nature of properly defining the critical or buckling load for composite plates with imperfections. (In the present case, the critical load may be defined[17] as the magnitude of the applied load at the point obtained from extrapolation of the prebuckling and the initial postbuckling paths of the end-shortening vs. applied load curve.) The results elucidate the nonlinear shear effect of the fiber composite material on global composite plate buckling and postbuckling responses, which are characterized by reduction in the buckling load and the postbuckling stiffness.

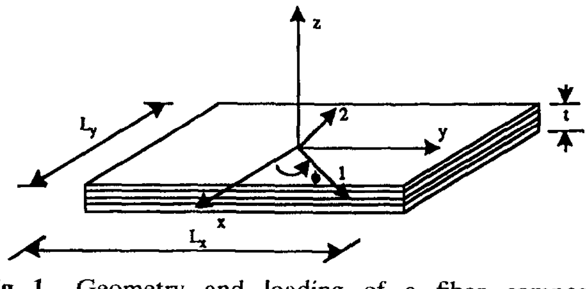

Fig. 1. Geometry and loading of a fiber composite laminate plate.

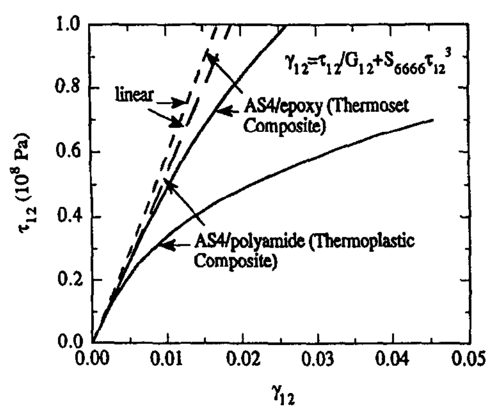

Fig. 2. In-plane shear stress-strain behavior of AS4/epoxy and AS4/polyamide composites.

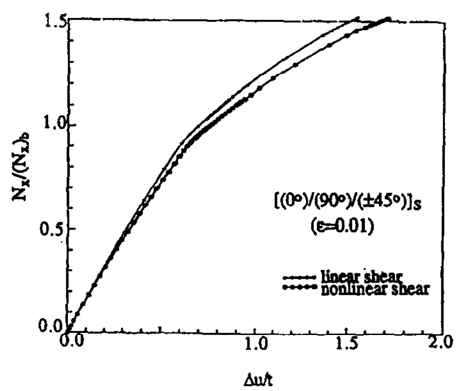

Fig. 3. End-shortening vs. applied load of $[(0°)/(90°)/(\pm 45°)]_S$ AS4/polyamide composite plate with imperfection (ε=0·01) subjected to uniaxial end compression.

3.2 Composite laminate shells under hydrostatic compression or axial end compression

In this section, cylindrical graphite-fiber/epoxy composite shells (Fig. 4) with two different ply lay-ups and fiber orientations, $[(0°)_2/(90°)_2]_s$ and $[(45°)/(-45°)]_{2S}$, subjected to hydrostatic compression, are analyzed. The ends of the shells are fixed to rigid plates to maintain their circular cross-sections, whereas rotations at the two ends are not restrained. In Section 3.2 (c), a cylindrical graphite/epoxy $[(45°)_2/(-45)_2]_S$ composite shell, subjected to external axial end compression, is considered. In this case, one end of the shell is fixed and the other end undergoes a uniform axial displacement. Effective composite ply properties of unidirectional graphite/epoxy given as follows are employed: E_{11}=138·0 GPa, E_{22}=14·5 GPa, ν_{12}=0·21, $G_{12}=G_{13}$=5·86 GPa, G_{23}=3·52 GPa, S_{6666}=7·32 $(\text{GPa})^{-3}$. The nonlinear shear stress-strain constitutive equation of the graphite/epoxy composite lamina depicted in Fig. 2 is used in the analyses. In the results given in this section, the end-shortening Δu is normalized by the laminate thickness t of the composite shell, and the applied load is normalized by the buckling load obtained from a linear bifurcation analysis.

(a) Cylindrical $[(0°)_2/(90°)_2]_S$ cross-ply composite laminate shell

The geometry of the cylindrical composite shell studied here is given as follows: L=25·4 cm, t=0·635 cm and D=25·4 cm. The eigenmode corresponding to the lowest eigenvalue, obtained from the linear bifurcation analysis, is used to introduce the geometric imperfection. Two values of the scaling parameter, i.e., ε=0·001 and 0·1, are used in the imperfection sensitivity study.

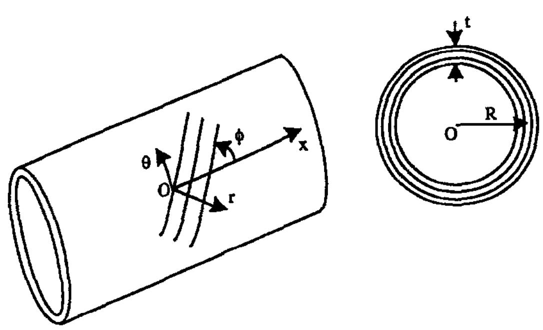

Fig. 4. Geometry and coordinates of a cylindrical fiber composite laminate shell.

During buckling and postbuckling deformations, the end-shortening vs. applied-load relationships of the cross-ply composite shells with linear and nonlinear ply constitutive properties are presented in Fig. 5(a) and (b). The deformed shapes of the shell at postbuckling states A and B in Fig. 5(a), with the given nonlinear shear relationship and ε=0·001, are shown in Fig. 6. In Fig. 5(a) the buckling load of the cross-ply composite shell with the imperfection ε=0·001 appears not significantly affected by the nonlinear composite constitutive properties. While the cylindrical composite shell with the linear material law displays less imperfection sensitivity, appreciable imperfection sensitivity is found during postbuckling deformations of the composite shell with nonlinear constitutive properties. Furthermore, the postbuckling load-bearing capacity of the composite shell with nonlinear shear constitutive properties is found to be lower than that of the linear case. In the case of ε=0·1, the end-shortening

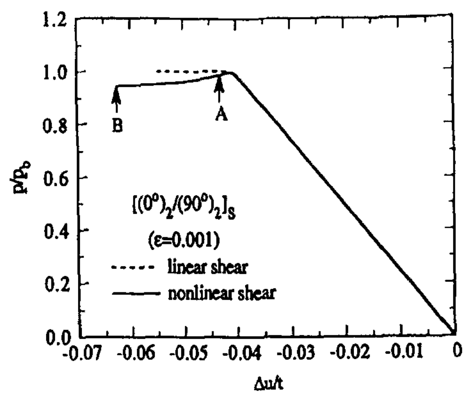

(a)

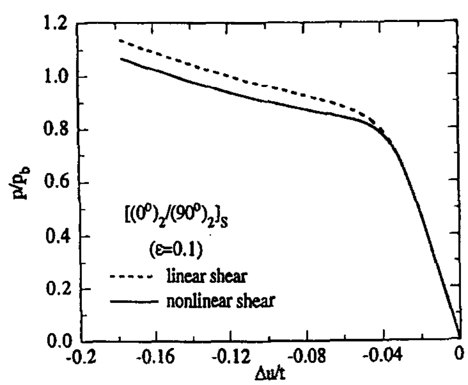

(b)

Fig. 5. End-shortening vs. applied load of $[(0°)_2/(90°)_2]_S$ AS4/epoxy composite cylindrical shells with imperfections subjected to hydrostatic compression (p_b=8·28 MPa); (a) ε=0·001; (b) ε=0·1.

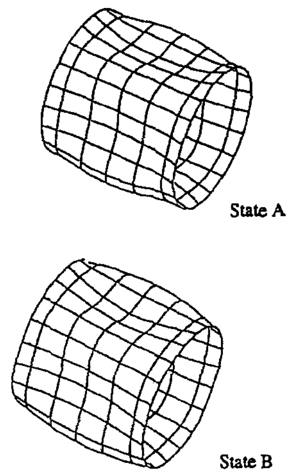

Fig. 6. Mode shapes of buckled $[(0°)_2/(90°)_2]_S$ AS4/epoxy composite shell at states A and B with imperfection (ε=0·001) subjected to hydrostatic compression (with nonlinear ply constitutive properties).

vs. applied-load curves in Fig. 5(b) reveal the nonlinear shear effect on the postbuckling deformations of the composite shells. Here the critical or buckling load of a composite shell with imperfections may be defined[17] as the magnitude of the applied load at which the minimum slope of the end-shortening vs. applied-load curve occurs. The composite shell follows a stable equilibrium postbuckling path, and the effect of material nonlinearity is manifested by the reduced postbuckling structural stiffness and lower load-bearing capacity.

(b) Cylindrical $[(45°)/(-45°)]_{2S}$ angle-ply composite laminate shell

The composite shell geometry used here is given as follows: L=20·32 cm, t=0·81 cm, and D=20·32 cm. Numerical results for buckling and postbuckling of the graphite/epoxy composite shells with the aforementioned linear and nonlinear constitutive properties under hydrostatic compression are shown in Fig. 7. The mode shapes of the buckled shell at the states A and B in Fig. 7 are shown in Fig. 8. It is interesting to note that the cylindrical angle-ply composite shell subjected to hydrostatic compression exhibits an appreciable end extension before buckling. In addition, completely different buckling and postbuckling mode shapes are predicted for the composite shells with the linear and the nonlinear ply constitutive equations. In the linear material case with ε=0·001, a snap-through is expected in the postbuckling region, whereas a global structural collapse failure mode with unbounded displacements is

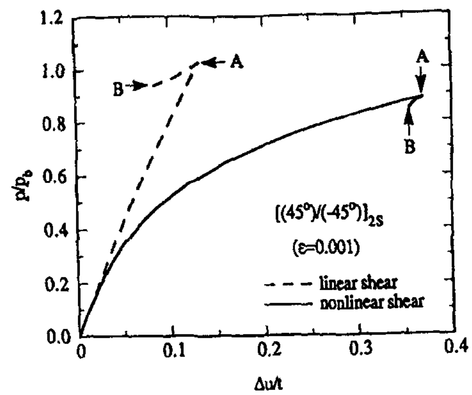

Fig. 7. End-shortening vs. applied load for $[(45°)/(-45°)]_{2S}$ AS4/epoxy composite cylindrical shell with imperfection subjected to hydrostatic compression (p_b=50·95 MPa).

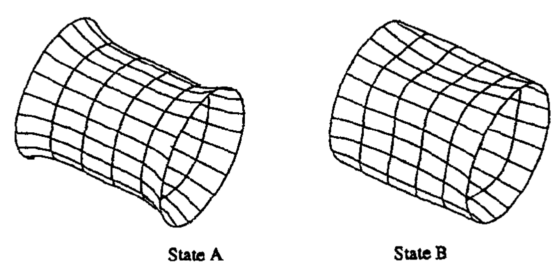

Fig. 8. Mode shapes of buckled $[(45°)/(-45°)]_{2S}$ AS4/epoxy composite shell at state A and B with imperfection (ε=0·001) subjected to hydrostatic compression (with nonlinear ply constitutive properties).

predicted for the composite shell with the aforementioned nonlinear material properties.

(c) Cylindrical composite laminate shells under axial end compression

In this section the effect of a different loading mode on the postbuckling response of a cylindrical composite shell is addressed. An angle-ply $[(45°)_2/(-45°)_2]_S$ graphite/epoxy, cylindrical laminate composite shell subjected to axial end compression is studied for illustration. The geometry, boundary conditions and the nonlinear shear stress-strain behavior of the composite lamina are the same as those used in Section 3.2 (a).

As in the previous case, the eigenmode corresponding to the lowest eigenvalue, obtained from a linear bifurcation analysis, is used to introduce the geometric imperfection. Two imperfection scaling parameters are used, i.e., ε=0·001 and ε=0·1, in the imperfection sensitivity study. The results obtained for the composite shells with linear and nonlinear material constitutive properties are presented in Fig. 9(a) and (b). Mode shapes of the buckled shells

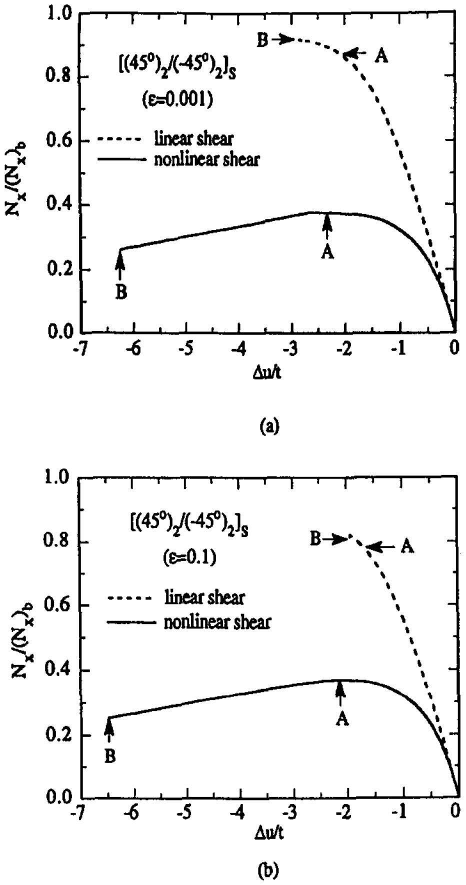

Fig. 9. End-shortening vs. applied load for $[(45°)_2/(-45°)_2]_S$ AS4/epoxy composite cylindrical shells with imperfections subjected to axial end compression ($(N_x)_b$=4·11 MN); (a) ε=0·001; (b) ε=0·1.

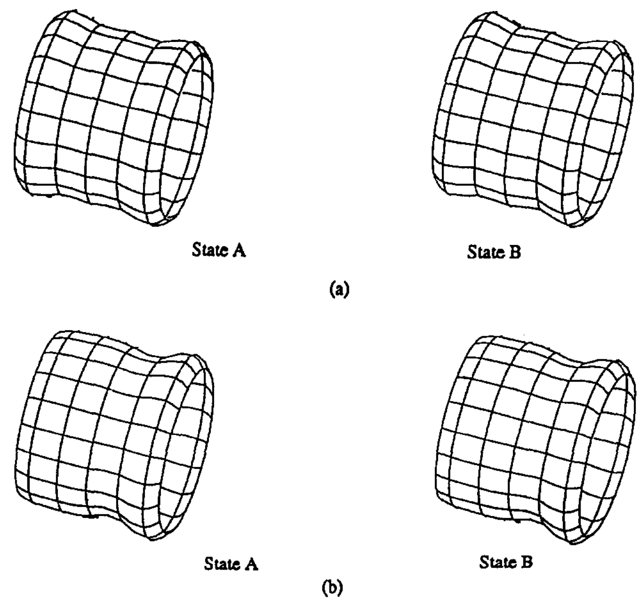

Fig. 10. Mode shapes of $[(45°)_2/(-45°)_2]_S$ AS4/epoxy composite shell with imperfection (ε=0·001) subjected to axial end compression (a) with linear ply constitutive properties; (b) with nonlinear ply constitutive properties.

under axial compression at states A and B (Fig. 9(a)), with the linear and nonlinear material properties and ε=0·001, are shown in Fig. 10(a) and (b) for illustration. As observed in Fig. 10(a), the composite laminate shell with linear constitutive properties is expected to exhibit a global structure collapse failure in an axisymmetric buckling mode shape. The composite shell with the nonlinear shear properties has significantly lower postbuckling structural stiffness than that with the linear material law. In addition, the cylindrical composite shell with the nonlinear material properties is predicted to collapse in a local postbuckling mode near the end of the shell — an obvious mode change in the postbuckling region from the linear case.

4 CONCLUSIONS

Based on the methods of analysis developed and the numerical results obtained in this study, the following conclusions may be drawn:

(1) The methods of analysis developed in this study are shown to be effective and efficient to address the coupled problem involving both composite material nonlinearity and geometrically structural nonlinearity (buckling, postbuckling), and their interactions.
(2) The composite material nonlinearity has significant effects on the geometrically nonlinear, structural buckling load, postbuckling structural stiffness, and structural failure mode shape of composite laminate plates and shells.
(3) The composite material nonlinearity also has an appreciable influence on the geometric imperfection sensitivity of composite structural buckling and postbuckling deformations.
(4) The degree of these effects mentioned in (2) and (3), due to the composite ply shear nonlinearity, on structural stability, load-bearing capability, and failure modes is dependent upon composite material lamination variables and lay-ups, structural geometry, and loading modes, as shown in various examples given in the paper.
(5) Quantitative determination of these nonlinear effects requires advanced computational nonlinear material and

structural mechanics analysis, such as the one given in Section 2 of this paper, due to the complexities of these coupled problems.

REFERENCES

1. Leissa, A. W., A review of recent developments in laminated composite plate buckling analysis. *Comp. Mat. Tech.*, ASME Petroleum Division, **45** (1992) 1–7.
2. Simitses, G. J., Buckling and postbuckling of imperfect cylindrical shells: a review. In *Proc. PV & P Conference and Exhibition on Nonlinear Analysis and NDE of Composite Material Vessels and Components*, (eds Hui, D. *et al.*), **115**. Chicago, Illinois, 20–24 July 1986, pp. 1–10.
3. Adams, D. F., Inelastic analysis of a unidirectional composite subjected to transverse normal loading. *J. Comp. Mat.*, **4** (1970) 310–328.
4. Hashin, Z., Bagchi, D., & Rosen, B. W., Nonlinear behavior of fiber composite laminates. *NASA Contractor Report NASA CR-2313*, 1974.
5. Kuppuswamy, T., Nanda, A. & Reddy, J. N., Materially nonlinear analysis of laminated composite plates. *Comp. Struct.*, **2** (1984) 315–328.
6. Tsai, S. W. & Hahn, H. T., Nonlinear elastic behavior of unidirectional composite laminae. *J. Comp. Mat.*, **7** (1973) 102–118.
7. Sun, C. T. & Chen, J. L., A simple flow rule for characterizing nonlinear behavior of fiber composites. *J. Comp. Mat.*, **23** (1989) 1009–1020.
8. Vaziri, R., Olson, M. D. & Anderson, D. L., Constitutive modeling of laminated fiber-reinforced composites. In *Proc. 5th International Conference on Composite Structures*, Elsevier Science Publishers, London, 1989, pp. 715–727.
9. Hahn, H. T., Nonlinear behavior of laminated composites. *J. Comp. Mat.*, **7** (1973) 257–271.
10. HajAli, R. & Wang, S. S., Nonlinear behavior of fiber composite materials and its effect on the postbuckling response of laminated plates. *Technical Report UIUC-NCCMR-90-10*, National Center for Composite Materials Research, University of Illinois, Urbana, Illinois, 1990.
11. Hu, H. T., Influence of in-plane shear nonlinearity on buckling and postbuckling responses of composite plates and shells. Presented at *The Winter Annual Meeting of ASME on Enhancing Analysis Techniques for Composite Materials*, **10**, ASME, (eds Schwer, L. *et al*)., Atlanta, Georgia, 1991, pp. 179–186.
12. Hu, H. T. & Wang, S. S., Effect of in-plane shear nonlinearity on buckling optimization of fiber-composite laminate shells. In *Proc. Eighth International Conference on Composite Materials* (ICCM/8), (eds Tsai, S. W. and Springer, G. S)., Honolulu, 15–19 July 1991, pp. 4-A-1–4-A-12.
13. Hu, H. T., Buckling analyses of fiber-composite laminate shells with material nonlinearity. *J. Comp. Tech. & Research*, **15** (1993) 202–208.
14. Anon., *ABAQUS User Manual*. Version 4-9, Hibbitt, Karlsson and Sorensen, Inc., Providence, RI, 1991.
15. Riks, E., An incremental approach to the solution of snapping and buckling problems. *Int. J. Solids & Struct.*, **15** (1979) 529–551.
16. Crisfield, M. A., A fast incremental/iterative solution procedure that handles 'snap-through'. *Computers & Struct.*, **13** (1982) 55–62.
17 Singer, J., Experimental techniques and comparison with theoretical results. In *Buckling and Post-Buckling; Lecture Notes in Physics*, No. 288, Springer-Verlag, Berlin, 1987.